の投与、無効な場合は病巣洗浄・掻爬。

8) 全身麻酔に関連した有害事象：

①アナフィラキシーショック：ステロイド剤等の投与。

②肝機能検査異常：肝庇護剤の投与。

③腎機能検査異常：輸液による電解質補正、重篤な場合は透析。

併用禁止薬

被験者において、試験前、試験期間中において併用禁止とする薬剤は特に規定しないが以下に挙げる薬剤は、心臓手術前後１週間の休薬が望ましい。

① パナルジン、プレタール等の抗血小板薬

② バイアスピリン

後療法

プロトコル治療後は一般的に難治性重症心不全患者に実施する標準治療を行う。つまり担当医が最善と判断する治療、すなわちリハビリテーション並びに合併症の防止を行い、特に制限を設けない。

予想される有害事象

心臓カテーテル検査に関連した有害事象、合併症

1) 鼠径穿刺部の疼痛、出血。
2) 局所麻酔薬によるアレルギー反応。
3) 術後の止血不良による穿刺部の血腫。
4) 極めて稀ではあるが術後穿刺部出血による後腹膜血腫。
5) 極めて稀ではあるが穿刺部の感染。

造影・心内圧検査による有害事象

1) 造影剤アレルギー。
2) 極めて稀ではあるが、カテーテル操作による心室、血管の穿孔。
3) 検査後の心タンポナーデ。
4) 房室ブロック（脚ブロックを含む）。
5) 心室性不整脈。
6) 極めて稀ではあるが死亡。
7) 感染症。

冠動脈内への幹細胞注入に関する有害事象

1) 培養上清中に細菌が検出され、同一の細菌により術部感染が発生した場合。
2) 細胞移植部からの腫瘍発生(間葉系幹細胞を体外で培養したのち、ヒトに投与した臨床試験はいくつか報告されているが、現在のところ腫瘍発生はない)。
3) 細胞移植時、冠動脈内注入する際に生じる心室性不整脈（前臨床試験ブタ全70頭への心筋局注に際し、初期の１例目においてのみ穿刺関連の心室性不整脈の発生を認めたが、穿刺前のアミオダロン前投薬によるプロトコル改変治療後は、心室性不整脈の発生は一例も認めていない)。

幹移植術後の心室性不整脈への対応について

これまでに報告された骨髄幹細胞の冠動脈内注入による臨床試験では、小児及び成人心不全を含め、致死性不整脈の発生は報告されていない。

一方、本研究で用いられる心臓内幹細胞については、心臓幹細胞自体の再生機序、gap-junction蛋白を介したホスト心筋との電気的融合の形成、前臨床試験での不整脈監視試験の結果からは、その心室性不整脈の発生の危険性は低いと思われる。また、最近報告された大型動物用いた類似の心臓内幹細胞移植の冠動脈注入法による前臨床試験においても、致死性不整脈の発生は認められていない。さらに、TICAP第１相臨床試験ならびに成人

虚血性心不全を対象にした SCIPIO や CADUCEUS 臨床試験のように、冠動脈注入法による不整脈惹起の報告もないことから、本第 2 相臨床試験において致死性不整脈の発生の可能性は低いと考えられる。

また、従来報告されている骨格筋芽細胞移植による催不整脈作用（心室性不整脈）と同様の不整脈発生の危険性に関して、日本循環器学会の不整脈治療のガイドラインに則り、標準的抗不整脈治療を行う。この抗不整脈治療に対して抵抗性の致死性不整脈の発生を認めた場合は、埋め込み型除細動器の移植適応ガイドラインに則り、適応とされる症例には埋め込み型除細動器の移植を行う。

<u>有害事象の報告と対応</u>

報告義務のある有害事象

報告義務のある有害事象は、初回の心臓カテーテル検査から幹細胞移植手術後 1 年の間に発生したものとする。

報告・対応手順

試験責任／分担医師は、一次報告（72 時間以内）、二次報告（7 日以内）、詳細調査報告、最終報告を行う。

対応手順

主任研究者、研究事務局および独立データモニタリング委員は、一次報告後の対応、二次報告後の対応、独立データモニタリング委員会による評価・勧告、対策の決定、最終報告後の対応を行う。

<u>臨床研究終了後の追跡調査</u>

3年間の臨床研究終了後も通常の保険診療行為として被験者の追跡を、10年以上を目安として行う。被験者に病原体感染等の有害事象が生じた場合は、適切な医療措置を行うとともに、最終調製物に関する確認を行い、原因究明に努める。他の被験者の健康状態も確認し、被験者の安全性確保に努める。

<u>観察・検査・報告項目とスケジュール</u>

心臓カテーテル検査当日　（細胞移植日）

1) 身体所見： 体重、血圧、脈拍数
2) 冠動脈造影： 主要冠動脈の有意狭窄の検証
3) 心機能　： 心内圧測定、心血管造影
4) 心電図
5) 24 時間心電図モニター監視　（術後から術後 1 週目まで）

心臓カテーテル検査翌日　（細胞移植後）

1) 身体所見： 体重、血圧、脈拍数
2) 血液学的検査：白血球数、好中球数、赤血球数、ヘマトクリット、ヘモグロビン、血小板
3) 生化学検査
   ① GOT(AST)、GPT(ALT)、LDH、総ビリルビン、直接ビリルビン、総タンパク、アルブミン、血清クレアチニン、BUN、電解質（Na、K、Cl）、CRP、CPK、CPK-MB、BS
4) 心電図
5) 胸部 X 線検査： 胸部前後撮影
6) 24 時間心電図モニター監視： 致死性・非致死性不整脈の検証

細胞移植後 1 週目

1) 身体所見： 体重、血圧、脈拍数
2) 血液学的検査：白血球数、好中球数、赤血球数、ヘマトクリット、ヘモグロビン、血小板
3) 生化学検査
   ① GOT(AST)、GPT(ALT)、LDH、総ビリルビン、直接ビリルビン、総タンパク、アルブミン、血清クレアチニン、BUN、電解質（Na、K、Cl）、CRP、CPK、CPK-MB、BS、BNP
4) 凝固系：PT、APTT、D-dimer
5) 24 時間心電図モニター監視： 致死性・非致死性不整脈の検証
6) 心電図
7) 胸部 X 線検査　： 胸部前後撮影
8) 臨床症状　　： 心不全、チアノーゼ

（倫理面への配慮）

遵守すべき諸規則

本研究に携わるすべての者は、ヒトを対象とする全ての医学研究が準拠すべき「世界医師会ヘルシンキ宣言」（1964年第18回世界医師会ヘルシンキ総会で起草、2004年10月第56回東京総会で最新改訂）や「臨床研究に関する倫理指針」（平成15年7月30日厚生労働省公布、改正：平成16年厚生労働省告示第459号）の内容を遵守し、更に「ヒト幹細胞を用いる臨床研究に関する指針」（平成18年7月3日 厚生労働省公布)の内容に準じて施行する。

説明と同意（インフォームド・コンセント）

試験責任／分担医師は、被験者が試験に参加する前、心臓組織の採取前及び細胞移植手術前に、それぞれ説明文書を用いて十分説明し、試験への参加について自由意思による同意を本人から文書として得る。文書による同意を得る際には、説明医師ならびに被験者が説明文書の内容を十分理解した上で、同意書（様式）に各自日付を記入し、記名捺印または署名する。試験責任／分担医師は、記名捺印または署名した同意書の写しを説明文書と共に被験者に交付し同意書原本は説明文書と共にカルテに添付して当該医療機関で保管する。

説明文書に重大な改訂があった場合、説明医師は試験参加中の被験者に対して改訂後の説明文書を用いて再度説明し、試験参加の継続について自由意思による同意を本人から文書として得る。

試験参加中の被験者が同意の撤回を申し出た場合、試験責任／分担医師はその旨をカルテに記載し、記録を残す。被験者は同意を撤回する場合、試験責任者に対し同意撤回文書の交付を要求し、必要事項を記入した後に、提出する。試験責任医師は同意撤回文書を独立データモニタリング委員会に提出報告する。独立データモニタリング委員会は同意撤回手続きが正しく行われたことを確認、担当の試験責任医師にこれを通知する。試験責任医師は被験者に通知し、同意撤回手続きが完了する．同時に試験責任医師は登録・データセンターに試験中止報告書を提出する。

個人情報の保護

個人情報の保護については、岡山大学に適用される法令、条例等を遵守する。試験に係わる関係者は、ヒト幹細胞臨床研究を行う上で知り得た被験者等に関する個人情報を正当な理由なく漏らしてはならないものとする。職を退いた後も同様とする。

試験責任医師および試験分担医師は、症例登録票および症例報告書等を当該機関外に提供する際には、連結可能匿名化を行うために新たに被験者識別コードを付し、それを用いる。医療機関外の者が、被験者を特定できる情報（氏名・住所・電話番号など）は記載しない。

登録・データセンターが医療機関へ照会する際の被験者の特定は、試験責任医師および試験分担医師が管理する被験者識別コードまたは登録・データセンターが発行した登録番号を用いて行う。主任研究者等が試験で得られた情報を公表する際には、被験者が特定できないよう十分配慮する。

健康被害に対する補償

本臨床試験の実施に起因して有害事象が発生し、被験者に健康被害が生じた時には、すみやかに適切な治療その他最善の措置を受けることが出来るように、主任研究者、試験分担医師と岡山大学病院が対応する。

C. 研究結果

本第2相臨床研究の開始以降、2014年4月までに、ランダム化により割振りされた細胞移植群10症例と非移植群のうち3か月目の評価検査を終了しかつ救済移植を希望された7症例の合計17症例に対して、患者さん由来の心臓内幹細胞の冠動脈内注入を実施した。移植細胞数はプロトコル通り体重kgあたり30万個の幹細胞を3等分し、右冠動脈、左前下行枝ならびに回旋枝内に選択的に合計3mLとなるように注入した。うち、解剖学的に低形成の冠動脈を示した3症例においては選択的注入を断念し残りの2本の冠動脈内にそれぞれ1.5mLずつ注入した。

一回当たりの冠動脈内注入時間は0.5～1.5分であったが、5分以上の休止期間をはさみ、全予定細胞数をそれぞれ冠動脈内に移植できた。右冠動脈起始部注入時に一過性の洞性徐脈を5症例に認め、バルーンによる1分以上の冠動脈閉塞の際には、ほぼ全症例において心電図上一過性のST-T変化と血圧の低下を観察した。これらの事象はバルーンdeflationにより速やかに基本調律やカテーテル前の心電図に回復し、持続的後療法を必要とする有害事象の発生は認めなかった。

また、プロトコル治療に則り不整脈予防のため、カテーテル後のアンカロン内服を全症例に実施しているが、うち2症例はアンカロンによる陰性変時作用により、1度の房室ブロックを術後2日目から検出し、同症例のアンカロン中止により速やかに房室ブロックの改善を認めた。また、1症例においては心臓手術後より投与開始されたワーファリンと移植手術中の抗凝固療法（ヘパリン）により、心臓カテーテル後一過性の脳内出血と脊椎内出血を認めたが、抗凝固療法の中止により回復した。全症例において細胞注入に伴う催不整脈作用を認めず、術後心タンポナーデ、感染症やアレルギーの合併も観察されなかった。

D. 考察

冠動脈注入法による心臓内幹細胞移植法は、安全で、これまでに経験した17症例において、心臓関連の有害事象の発生は認められなかった。有効性検証は現在症例登録実施中であるが、これまで移植した17症例のうち、3か月目の評価カテーテル検査を終了した11症例に関しては、非移植群の7症例に比べ統計学的に有意に心機能は改善していた(p=0.03)。今後、予定症例数の34人まで継続的に細胞移植を実施し、カテーテル治療の安全性と細胞治療の有効性についてより詳細に検討していく。

E. 結論

冠動脈内注入法による心臓内幹細胞移植は、技術的に実施可能で安全である。本臨床研究開始初年度内に予定症例数の50%に当たる17人に移植できたことにより、研究計画2年目に全予定症例数に移植することが充分可能であり、臨床治験に向けた細胞移植における安全性及び有効性に関する臨床的エビデンス構築の推進を今後も継続していく。

F. 健康危険情報

該当なし。

G. 研究発表

1. 論文発表

① Ohno N, Ohtsuki S, Kataoka K, Baba K, Okamoto Y, Kondo M, Sano S, Kasahara S, Honjo O, Morishima T. Usefulness of balloon angioplasty for the right ventricle-pulmonary artery shunt with the

modified Norwood procedure. Catheter Cardiovasc Interv. 2013 Apr;81(5):837-42.

2. 学会発表

① Baba, K. Ohtsuki. S : Pulmonary flow control using balloon angioplasty for right ventricular-pulmonary artery shunt with a hemoclip in Hypoplastic left heart syndrome. Pediatric and adult interventional cardiac symposium, Florida, (6.8.2013)

② 馬場 健児[1], 大月 審一[1], 岡本 吉生[1], 近藤 麻衣子[1], 栗田 佳彦[1], 栄徳 隆裕[1], 小寺 亜矢[1], 笠原 真悟[2], 佐野 俊二[2], 岩崎 達雄[3], 森島 恒雄[4] [1] 岡山大学病院 小児循環器科, [2] 岡山大学大学院医歯薬総合研究科 心臓血管外科学, [3] 岡山大学大学院医歯薬総合研究科 麻酔・蘇生学, [4] 岡山大学大学院医歯薬総合研究科 小児医科学：Hemoclipとballoon angioplastyを組み合わせたNorwood術後の肺血流コントロール：第24回JPIC学術集会 愛媛 (1.25.2013)

③ 近藤 麻衣子[1], 大月 審一[1], 馬場 健児[1], 岡本 吉生[1], 栗田 佳彦[1], 栄徳 隆裕[1], 小寺 亜矢[1], 佐野 俊二[2], 笠原 真悟[2], 岩崎 達雄[3], 戸田 雄一郎[3], 清水 一好[3] [1] 岡山大学病院 小児循環器科, [2] 岡山大学大学院医歯薬総合研究科 心臓血管外科, [3] 岡山大学大学院医歯薬総合研究科 麻酔蘇生科：clip付きBTshuntに対するバルーン拡大術の有用性：第24回JPIC学術集会 愛媛 (1.25.2013)

④ 栄徳 隆裕, 大月 審一, 馬場 健児, 岡本 吉生, 近藤 麻衣子, 栗田 佳彦, 小寺 亜矢 岡山大学病院 小児循環器科：カテーテルインターベンションによって完全閉塞した肺動脈やshuntを再開通させる効果について：第24回JPIC学術集会 愛媛 (1.25.2013)

⑤ 栗田 佳彦[1], 大月 審一[1], 小寺 亜矢[1], 栄徳 隆裕[1], 近藤 麻衣子[1], 岡本 吉生[1], 馬場 健児[1], 森嶋 恒雄[2], 佐野 俊二[3], 笠原 真吾[3], 岩崎 達雄[4], 戸田 雄一郎[4] [1] 岡山大学病院 小児循環器科, [2] 岡山大学大学院医歯薬総合研究科 小児医科学, [3] 岡山大学病院 心臓血管外科, [4] 岡山大学病院 麻酔・蘇生科：心房中隔・fenestrationに対するstent留置術：第24回JPIC学術集会 愛媛 (1.26.2013)

⑥ 大月 審一[1], 馬場 健児[1], 岡本 吉生[1], 栗田 佳彦[1], 近藤 麻衣子[1], 栄徳 隆裕[1], 小寺 亜矢[1], 森島 恒雄[2] [1] 岡山大学病院 小児循環器科, [2] 岡山大学大学院医歯薬総合研究科 小児医科学：ASD with Deficient Rim：小児例における適応と試み：第24回JPIC学術集会 シンポジウム 愛媛 (1.26.2013)

⑦ 栗田 佳彦[1], 大月 審一[1], 栄徳 隆裕[1], 近藤 麻衣子[1], 大野 直幹[1], 馬場 健児[1], 森嶋 恒雄[2], 佐野 俊二[3], 笠原 真吾[3], 岩崎 達雄[4], 戸田 雄一郎[4] [1] 岡山大学病院 小児循環器科, [2] 岡山大学大学院医歯薬総合研究科 小児医科学, [3] 岡山大学病院 心臓血管外科, [4] 岡山大学病院 麻酔・蘇生科：当院での術中肺静脈ステント症例の検討：第 49 回日本小児循環器学会学術集会 東京 (7.11.2013)

⑧ 馬場 健児[1], 大月 審一[1], 栄徳 隆裕[1], 栗田 佳彦[1], 近藤 麻衣子[1], 大野

直幹[1], 森嶋 恒雄[2], 佐野 俊二[3], 笠原 真吾[3], 岩崎 達雄[4], 戸田 雄一郎[4] [1] 岡山大学病院 小児循環器科, [2] 岡山大学大学院医歯薬総合研究科 小児医科学, [3] 岡山大学病院 心臓血管外科, [4] 岡山大学病院 麻酔・蘇生科：両側肺動脈 banding 後 Norwood 手術と初回 Norwood 手術との肺動脈成長に関する検討：第 49 回日本小児循環器学会学術集会 東京 (7.11.2013)

H. 知的財産の出願・登録状況

1. 特許取得

該当なし。

2. 実用新案登録

該当なし。

3. その他

該当なし。

研究成果の刊行に関する一覧表

書籍（王　英正）

著者氏名	論文タイトル名	書籍全体の編集者名	書　籍　名	出版社名	出版地	出版年	ページ
樽井俊、佐野俊二、王　英正	心筋幹細胞を用いた先天性心疾患に対する心筋再生医療	福田恵一	月刊循環器	医学出版	東京	2013	69-76

書籍（佐野俊二）

著者氏名	論文タイトル名	書籍全体の編集者名	書　籍　名	出版社名	出版地	出版年	ページ
黒子洋介、佐野俊二	先天性心疾患 完全大血管転位症	井上　博、許　俊鋭、檜垣實男、代田浩之、筒井裕之	今日の循環器疾患	医学書院	東京	2013	531-532
服部　滋、吉積　功、川畑拓也、新井禎彦、笠原真悟、佐野俊二	先天性右室瘤の外科治療：乳児期に急速な瘤拡大を示した1例	中西敏雄	日本小児循環器学会雑誌	株式会社協和企画	東京	2013	194-199
樽井俊、佐野俊二、王　英正	心筋幹細胞を用いた先天性心疾患に対する心筋再生医療	福田恵一	月刊循環器	医学出版	東京	2013	69-76

雑誌（王　英正）

発表者氏名	論文タイトル名	発表誌名	巻号	ページ	出版年
Ogata T, Naito D, Nakanishi N, Hayashi YK, Taniguchi T, Miyagawa K, Hamaoka T, Maruyama N, Matoba S, Ikeda K, Yamada H, Oh H, Ueyama T.	MURC/Cavin-4 facilitates recruitment of ERK to caveolae and concentric cardiac hypertrophy induced by α1-adrenergic receptors.	*Proc Natl Acad Sci U S A.*	111	3811-3816	2014

Tarui S, Sano S, Oh H.	Stem cell therapy in patients with single ventricle physiology.	*Methodist DeBakey Cardiovascular Journal*,	in press		2014

雑誌（佐野俊二）

発表者氏名	論文タイトル名	発表誌名	巻号	ページ	出版年
Takaya Y, Taniguchi M, Akagi T, Nobusada S, Kusano K, Ito H, Sano S.	Long-term effects of transcatheter closure of atrial septal defect on cardiac remodeling and exercise capacity in patients older than 40 years with a reduction in cardiopulmonary function	*J Interv Cardiol*	26	195-199	2013
Ohno N, Ohtsuki S, Kataoka K, Baba K, Okamoto Y, Kondo M, Sano S, Kasahara S, Honjo O, Morishima T	Usefulness of balloon angioplasty for the right ventricle-pulmonary artery shunt with the modified Norwood procedure	*Catheter Cardiovasc Interv*	81	837-842	2013
Tarui S, Sano S, Oh H.	Stem cell therapy in patients with single ventricle physiology.	*Methodist DeBakey Cardiovascular Journal*,	in press		2014
Takaya Y, Akagi T, Kijima Y, Nakagawa K, Taniguchi M, Ohtani H, Sano S, Ito H.	Transcatheter closure of right-to-left atrial shunt in patients with platypnea-orthodeoxia syndrome associated with aortic elongation.	*Cardiovasc Interv Ther.*	Epub ahead of print		2014
Ündar A, Wang S, Palanzo D, Weaver B, Pekkan K, Agirbasli M, Zahn JD, Luciani GB, Clark JB, Wilson RP, Kunselman AR, Sano S, Belli E, Pierce WS, Myers JL.	Outcomes of the ninth international conference on pediatric mechanical circulatory support systems and pediatric cardiopulmonary perfusion.	*Artif Organs.*	38	5-10	2014

Sano S, Fujii Y, Kasahara S, Kuroko Y, Tateishi A, Yoshizumi K, Arai S.	Repair of Ebstein's anomaly in neonates and small infants: impact of right ventricular exclusion and its indications.	*Eur J Cardiothorac Surg.*	45	549-555	2014
Tateishi A, Kasahara S, Kawabata T, Kuroko Y, Yoshizumi K, Takagaki M, Arai S, Sano S.	The effect of pulmonary root translocation on the left ventricular outflow tract.	*Ann Thorac Surg.*	96	1469-1471	2013
Kijima Y, Akagi T, Nakagawa K, Taniguchi M, Ueoka A, Deguchi K, Toh N, Oe H, Kusano K, Sano S, Ito H.	Catheter closure of patent foramen ovale in patients with cryptogenic cerebrovascular accidents: initial experiences in Japan.	*Cardiovasc Interv Ther.*	29	11-17	2014
Kanamitsu H, Fujii Y, Mitsui H, Sano S.	Effects of atrial natriuretic peptide after prolonged hypothermic storage of the isolated rat heart.	*Artif Organs.*	37	1003-1008	2013

雑誌（大月審一）

発表者氏名	論文タイトル名	発表誌名	巻号	ページ	出版年
Ohno N, Ohtsuki S, Kataoka K, Baba K, Okamoto Y, Kondo M, Sano S, Kasahara S, Honjo O, Morishima T.	Usefulness of balloon angioplasty for the right ventricle-pulmonary artery shunt with the modified Norwood procedure.	*Catheter Cardiovasc Interv.*	81	837-842	2013

MURC/Cavin-4 facilitates recruitment of ERK to caveolae and concentric cardiac hypertrophy induced by α1-adrenergic receptors

Takehiro Ogata[a], Daisuke Naito[a], Naohiko Nakanishi[a], Yukiko K. Hayashi[b], Takuya Taniguchi[a], Kotaro Miyagawa[a], Tetsuro Hamaoka[a], Naoki Maruyama[a], Satoaki Matoba[a], Koji Ikeda[a], Hiroyuki Yamada[a], Hidemasa Oh[c], and Tomomi Ueyama[a,1]

[a]Department of Cardiovascular Medicine, Graduate School of Medical Science, Kyoto Prefectural University of Medicine, Kyoto 602-8566, Japan; [b]Department of Neurophysiology, Tokyo Medical University, Tokyo 160-8402, Japan; and [c]Department of Regenerative Medicine, Center for Innovative Clinical Medicine, Okayama University Hospital, Okayama 700-8558, Japan

Edited by J. G. Seidman, Harvard Medical School, Boston, MA, and approved February 3, 2014 (received for review August 13, 2013)

The actions of catecholamines on adrenergic receptors (ARs) induce sympathetic responses, and sustained activation of the sympathetic nervous system results in disrupted circulatory homeostasis. In cardiomyocytes, α1-ARs localize to flask-shaped membrane microdomains known as "caveolae." Caveolae require both caveolin and cavin proteins for their biogenesis and function. However, the functional roles and molecular interactions of caveolar components in cardiomyocytes are poorly understood. Here, we showed that muscle-restricted coiled-coil protein (MURC)/Cavin-4 regulated α1-AR–induced cardiomyocyte hypertrophy through enhancement of ERK1/2 activation in caveolae. MURC/Cavin-4 was expressed in the caveolae and T tubules of cardiomyocytes. MURC/Cavin-4 overexpression distended the caveolae, whereas MURC/Cavin-4 was not essential for their formation. MURC/Cavin-4 deficiency attenuated cardiac hypertrophy induced by α1-AR stimulation in the presence of caveolae. Interestingly, MURC/Cavin-4 bound to α1A- and α1B-ARs as well as ERK1/2 in caveolae, and spatiotemporally modulated MEK/ERK signaling in response to α1-AR stimulation. Thus, MURC/Cavin-4 facilitates ERK1/2 recruitment to caveolae and efficient α1-AR signaling mediated by caveolae in cardiomyocytes, which provides a unique insight into the molecular mechanisms underlying caveola-mediated signaling in cardiac hypertrophy.

caveola | signal transduction | heart | plasma membrane

Caveolae are plasmalemmal invaginations enriched in cholesterol, glycosphingolipids, and lipid-anchored proteins relative to the bulk of the plasma membrane (1, 2). Owing to their specific lipid composition, caveolae concentrate several signaling molecules involved in cellular processes or trafficking events from the cell surface; therefore, they are recognized as a platform for preassembled complexes of receptors, signal components, and their targets, facilitating efficient and specific cellular responses (3–5). Accumulating evidence has demonstrated that caveola biogenesis and function depend on two distinct caveolar components: caveolins and cavins (6, 7). Caveolin (Cav)-1 and Cav-2 are expressed in most cell types, including adipocytes, endothelial cells, fibroblasts, and smooth myocytes, whereas Cav-3 is expressed exclusively in smooth, skeletal, and cardiac myocytes. Caveolin deficiency leads to caveolar loss, which is accompanied by alterations in signaling responses (8, 9). Cavins are also structural components of caveolae and assume four isoforms, namely, polymerase I and transcript release factor (PTRF)/Cavin-1, serum deprivation protein response (SDPR)/Cavin-2, SDR-related gene product that binds to C kinase (SRBC)/Cavin-3, and muscle-related coiled-coil protein (MURC) (6), which is also known as "Cavin-4" because of its sequence homology with other cavins and localization to the caveolae (10). Previously, we reported the association of MURC/Cavin-4 with SDPR/Cavin-2 and identified MURC/Cavin-4 mutations in dilated cardiomyopathy patients (11, 12). PTRF/Cavin-1 and SDPR/Cavin-2 are expressed in various cell types, including myocytes (10, 11), and SRBC/Cavin-3 is expressed in many cell types except for muscle cells (13), whereas MURC/Cavin-4 is expressed exclusively in myocytes, similar to Cav-3 (11). Recent studies have shown that cavins and caveolins form a complex, called the "caveolin–cavin complex," which modifies caveolar biogenesis and function (14, 15). PTRF/Cavin-1 and SDPR/Cavin-2 are required for caveolar invagination and SRBC/Cavin-3 for caveolar budding to form caveolar vesicles (13, 16, 17). However, the functional role of MURC/Cavin-4 in caveolar morphology is not known.

Alpha-1 adrenergic receptors (α1-ARs) are members of the G protein-coupled receptor (GPCR) family and have been demonstrated to accumulate in caveolar fractions of the myocardium (5). GPCRs are well-known representatives of receptors concentrated in caveolae and transduce several signals from substrates to downstream effectors in caveolae (18). Because disruption of the caveolae affects the response to several GPCRs, caveolae are considered important plasma membrane structures that coordinate GPCRs and their downstream signaling components (5). In our previous study, we showed that MURC/Cavin-4 knockdown suppressed α1-AR agonist-induced atrial natriuretic peptide expression and myofibrillar organization in cardiomyocytes and that transgenic mice overexpressing MURC/Cavin-4 in cardiac tissue

Significance

Caveolae are recognized as a platform for preassembled complexes of receptors, signal components, and their targets, facilitating efficient and specific cellular responses at the plasma membrane. ERK is activated at the plasma membrane and an important molecule that has been well studied for its integral role in signal transduction events during physiological adaptation and pathological manifestation. Here we show that although muscle-restricted coiled-coil protein (MURC)/Cavin-4, a muscle-specific caveola component, is dispensable for caveolar formation in cardiomyocytes, MURC/Cavin-4 serves as an ERK-recruiting protein in the caveolae within cardiomyocytes. The recruiting function of MURC/Cavin-4 is necessary to elicit efficient signaling of the α1-adrenergic receptor–ERK cascade in concentric cardiac hypertrophy. Our findings provide unique insight into the molecular mechanisms underlying caveola-mediated signaling in cardiac hypertrophy.

Author contributions: T.O. and T.U. designed research; T.O., D.N., N.N., T.T., K.M., T.H., and N.M. performed research; T.O., Y.K.H., S.M., K.I., H.Y., H.O., and T.U. analyzed data; and T.O. and T.U. wrote the paper.

The authors declare no conflict of interest.

This article is a PNAS Direct Submission.

[1]To whom correspondence should be addressed. E-mail: toueyama-circ@umin.ac.jp.

This article contains supporting information online at www.pnas.org/lookup/suppl/doi:10.1073/pnas.1315359111/-/DCSupplemental.

(MURC-Tg) developed cardiomyocyte hypertrophy at 5 wk of age (11). These results suggest that MURC/Cavin-4 is involved in α1-AR signaling and cardiac hypertrophy.

In the present study, we manipulated MURC/Cavin-4 expression to investigate the role of MURC/Cavin-4 in caveolar morphology and α1-AR–induced cardiac hypertrophy. Overexpression and deletion of MURC/Cavin-4 showed the roles of MURC/Cavin-4 in the caveolar morphology of cardiomyocytes. Furthermore, we found that MURC/Cavin-4 facilitated ERK1/2 recruitment to caveolae and ERK activation in α1-AR–induced concentric cardiomyocyte hypertrophy.

Results

MURC/Cavin-4 Forms Caveolin–Cavin Complexes in the Caveolae and T Tubules and Modulates Caveolar Morphology in Cardiomyocytes. To reveal the functional significance of MURC/Cavin-4 as a caveolar component in cardiomyocytes, we examined the association of MURC/Cavin-4 with other cavins and caveolins. Expression plasmids encoding MURC/Cavin-4, Cav-3, and PTRF/Cavin-1 were transfected into CV-1 (simian) in origin, and carrying the SV40 genetic material (COS) cells, a fibroblast-like cell line derived from monkey kidney tissue. Immunoblot analysis showed that MURC/Cavin-4 was coimmunoprecipitated with Cav-3 and PTRF/Cavin-1 (Fig. S1 *A* and *B*). MURC-HA and Cav-3-T7 expressions were not reduced in supernatants immunoprecipitated by anti-T7 and anti-HA antibodies, respectively (Fig. S1*A*), whereas MURC-FLAG expression was reduced in the supernatant immunoprecipitated by the anti-HA antibody, although PTRF/Cavin-1-HA expression was not reduced in the supernatant immunoprecipitated by the anti-FLAG antibody (Fig. S1*B*). These results suggest that MURC/Cavin-4 binds to PTRF/Cavin-1 with high affinity, and that MURC/Cavin-3 does not entirely bind to Cav-3.

The bimolecular fluorescence complementation (BiFC) assay confirmed that MURC/Cavin-4, Cav-3, PTRF/Cavin-1, and SDPR/Cavin-2 interact in living cardiomyocytes (Fig. S1 *C* and *D*). Immunoelectron microscopy revealed that MURC/Cavin-4 was expressed in caveolae and T tubules in cardiomyocytes of adult mice (Fig. 1*A*). These observations are in accordance with our previous finding showing that MURC/Cavin-4 was localized to the Z line in cardiomyocytes (11) because the T-tubule system is in register with the Z lines and the immunostaining pattern of Cav-3 has been shown to coincide with the Z line in the heart (19). Because it was confirmed that MURC/Cavin-4 was expressed by caveolae, we assessed whether MURC/Cavin-4 affected caveolar morphology in cardiomyocytes. In cardiomyocytes of 13-wk-old MURC-Tg mice, the caveolae were significantly distended compared with those of wild-type (WT) mice (Fig. 1*B*). The effects of MURC/Cavin-4 on caveolae were supported by the results of an in vitro study in which MURC/Cavin-4 overexpression significantly increased the caveolar area and perimeter in cardiomyocytes compared with β-galactosidase (LacZ) overexpression (Fig. 1*C*). These results indicated that MURC/Cavin-4 modified the morphology of formed caveolae in cardiomyocytes.

MURC/Cavin-4 Is Associated with α1-ARs at Caveolae in Cardiomyocytes. We next investigated the localization of α1-ARs in cardiomyocytes. α1-AR exists as three molecular subtypes: α1A, -B. and -D. The α1A and -B subtypes are expressed in the myocardium, whereas the α1D subtype is expressed in vascular muscle (20). Because antibodies for α1-AR subtypes, which are frequently cited, have been shown to be nonspecific (21), we used plasmids encoding red fluorescent protein mCherry-conjugated α1A-AR (ADRA1A) and α1B-AR (ADRA1B). ADRA1A and ADRA1B signals were observed predominantly at the plasma membrane and partly within the cytoplasm (Fig. 2*A*). ADRA1A and ADRA1B signals were colocalized with endogenous Cav-3 and MURC/Cavin-4 at the plasma membrane and partly within the cytoplasm. Immunoprecipitation and BiFC assays revealed that both ADRA1A and ADRA1B were bound to MURC/Cavin-4 in COS cells and cultured rat cardiomyocytes, respectively (Fig. 2 *B* and *C*).

Because Cav-3 has also been demonstrated to bind to α1-ARs (22), we investigated whether Cav-3 could influence the localization of MURC/Cavin-4 and α1-ARs in cardiomyocytes. Cav-3 knockdown impaired the plasma membrane localization of MURC/Cavin-4, resulting in the accumulation of MURC/Cavin-4 in the cytosol of cardiomyocytes (Fig. S2 *A*–*C*). However, α1-ARs were retained at the plasma membrane in Cav-3–knocked down cardiomyocytes (Fig. S2*A*).

MURC/Cavin-4 Deficiency Attenuates α1-AR–Induced ERK Activation and Cardiac Hypertrophy. The above-mentioned observations that α1-ARs bound to MURC/Cavin-4 at caveolae in cardiomyocytes led us to examine whether MURC/Cavin-4 influenced the response to α1-AR stimulation in vivo. To this end, we subjected WT and

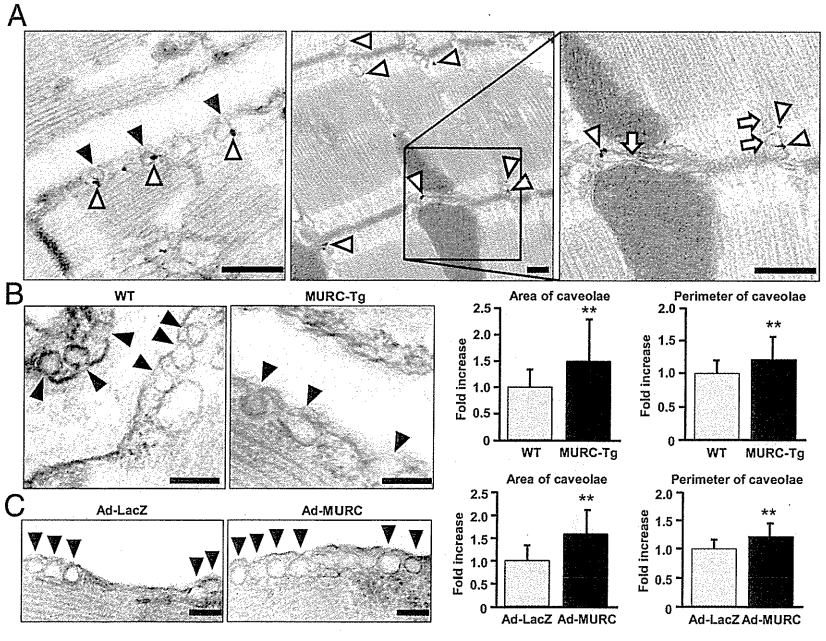

Fig. 1. MURC/Cavin-4 exists in the caveolae and T tubules and modulates caveolar morphology in cardiomyocytes. Representative electron microscopic images of mouse heart tissue and adult cultured cardiomyocytes. (*A*) Immunogold staining of MURC/Cavin-4 (white arrowheads) was observed at caveolae (black arrowheads) and T tubules (white arrows) of cardiomyocytes. (*B* and *C*) Representative shapes of caveolae in mouse heart tissue (*B*, *Left*) and rat cultured cardiomyocytes with or without MURC/Cavin-4 overexpression (*C*, *Left*). Caveolae were identified by their characteristic flask shapes and locations at or near the plasma membrane. Relative caveolar areas and perimeters were measured in cardiomyocytes from heart tissue (*B*, *Right*) and cultured cardiomyocytes (*C*, *Right*). Data are presented as mean ± SEM. $^{**}P < 0.01$ compared with controls. (Scale bars: 500 nm in *A*; and 200 nm in *B* and *C*.)

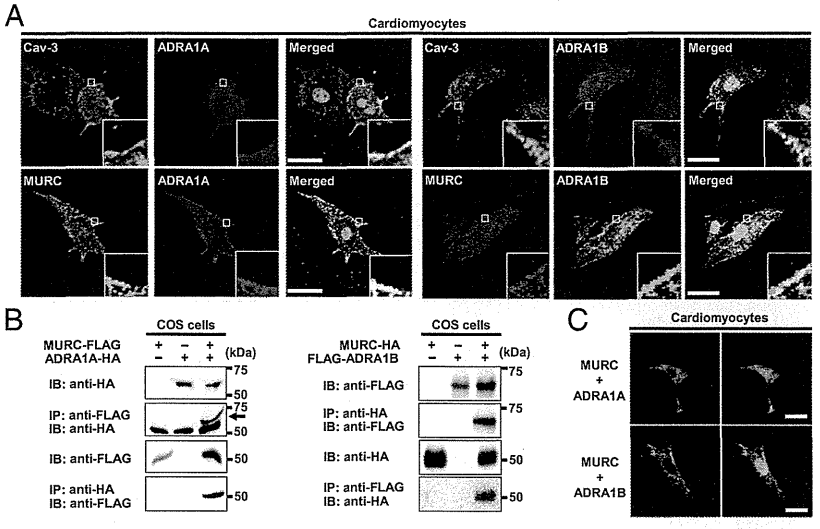

Fig. 2. MURC/Cavin-4 is associated with α1-ARs at caveolae in cardiomyocytes. (*A*) Representative fluorescence images of rat neonatal cardiomyocytes. Cardiomyocytes were cotransfected with ADRA1A- or ADRA1B-pmCherry. MURC/Cavin-4 and Cav-3 were costained with ADRA1A and ADRA1B (white boxes). (*B*) COS cells were transfected with MURC/Cavin-4-FLAG and/or ADRA1A-HA (*Left*), or with MURC/Cavin-4-HA and/or FLAG-ADRA1B (*Right*). The black arrow indicates ADRA1A-HA. (*C*) In situ association of MURC/Cavin-4 with α1-ARs in living cardiomyocytes was confirmed using the BiFC assay. Cardiomyocytes were cotransfected with phmKGC-MN-MURC and phmKGN-MN-ADRA1A or phmKGN-MN-ADRA1B. Nuclei were stained with DAPI (blue). (Scale bars: 20 μm in *A* and *C*.) IB, immunoblots; IP, immunoprecipitation. mKGC, monomeric Kusabira Green.

MURC/Cavin-4–null (*MURC*$^{-/-}$) mice (Fig. S3 *A* and *B*) to α1-AR–induced cardiac hypertrophy. *MURC*$^{-/-}$ mice are fertile, exhibit normal growth under normal conditions (Fig. S3*C*), and are indistinguishable by cardiac mass and function from WT mice under physiological conditions (Tables S1 and S2). Furthermore, caveolae and Cav-3 localization at the plasma membrane are retained in cardiomyocytes of *MURC*$^{-/-}$ mice (Fig. S3 *D* and *E*), indicating that MURC/Cavin-4 is not essential to the membrane localization of Cav-3 and caveola formation in cardiomyocytes. Phenylephrine (PE) infusion for 7 d caused marked concentric cardiac hypertrophy in WT mice, whereas MURC/Cavin-4 depletion suppressed cardiac hypertrophy, as evaluated using a cross-sectional area (Fig. 3*A*). Morphological and echocardiographic analyses also showed attenuated cardiac hypertrophy in *MURC*$^{-/-}$ mice (Tables S1 and S2). In the hearts of *MURC*$^{-/-}$ mice, BNP and βMHC mRNA expression levels were reduced in response to PE, compared with those of WT mice (Fig. 3*B*). A previous study demonstrated that, in ADRA1A and ADRA1B double-knockout (KO) (α1AB-KO) mice, ERK activation was reduced and PE could not activate ERK in cardiomyocytes, resulting in a reduced heart size in α1AB-KO mice compared with that in male WT mice (23). Therefore, we investigated ERK activation in WT and *MURC*$^{-/-}$ hearts. After PE infusion for 2 d, ERK activation was significantly suppressed in the hearts of *MURC*$^{-/-}$ mice compared with WT mice (Fig. 3*C*). In neonatal mouse cardiomyocytes isolated from WT and *MURC*$^{-/-}$ mice, PE-induced ERK activation was also significantly suppressed in *MURC*$^{-/-}$ cardiomyocytes compared with the level in WT cardiomyocytes (Fig. S3*F*). Mitogen-activated protein kinases (MAPKs), including ERK1/2, modulate cardiac hypertrophy through G proteins (24). Therefore, we assessed p38 and JNK activities in the hearts of WT and *MURC*$^{-/-}$ mice (Fig. S3*G*). The basal activity of p38 did not differ between WT and *MURC*$^{-/-}$ hearts, whereas JNK activation was significantly increased in *MURC*$^{-/-}$ hearts compared with the level in WT hearts. However, both p38 and JNK activities were not enhanced by PE infusion in the hearts of WT and *MURC*$^{-/-}$ mice.

MURC/Cavin-4 Serves as an ERK-Recruiting Protein in the Caveolae and Modulates α1-AR–Induced Hypertrophic Responses in Cardiomyocytes. To clarify the molecular mechanisms responsible for MURC/Cavin-4–mediated cardiac hypertrophy, we knocked down MURC expression in neonatal rat cardiomyocytes. PE increased MURC/Cavin-4 mRNA expression in cardiomyocytes, whereas MURC/Cavin-4 RNA interference (RNAi) using Ad-rMURC short hairpin RNA (shRNA) attenuated PE-induced MURC/Cavin-4 mRNA expression (Fig. S4*A*). MURC/Cavin-4 RNAi reduced PE-induced increases in cell size and BNP mRNA expression (Fig. S4 *B* and *C*), which is consistent with the in vivo study described above. PE-induced ERK activation was also suppressed in neonatal rat cardiomyocytes infected with Ad-MURC-shRNA as well as mouse cardiomyocytes isolated from *MURC*$^{-/-}$ mice (Fig. 4*A*). In cardiomyocytes infected with Ad-Luc-shRNA, ERK activation was detected 5 min after PE stimulation, which peaked at 30 min and then declined, whereas in cardiomyocytes infected with Ad-MURC-shRNA, ERK activation peaked at 5 min and then declined, which was significantly suppressed compared with that in Ad-Luc-shRNA–infected cardiomyocytes, suggesting that MURC/Cavin-4 plays a determinant role in the modulation of signaling amplitude and the duration of ERK activation in response to PE stimulation.

A previous study using immunoelectron microscopy showed that ERK was concentrated in caveolae (25). ERK is activated at the plasma membrane by several GPCRs and subsequently translocates to the nucleus and cytoplasm (26). Therefore, we investigated the functional role of MURC/Cavin-4 in ERK localization. In unstimulated cardiomyocytes, total and phosphorylated ERK was distributed throughout the cytoplasm and partially at the plasma membrane, where it was colocalized with MURC (Fig. 4*B*). Upon PE stimulation, both MURC/Cavin-4 and phosphorylated ERK were translocated from the plasma membrane to the perinuclear region (Fig. 4 *B* and *C*). MURC/Cavin-4 knockdown reduced phosphorylated ERK accumulation at the plasma membrane (Fig. 4*D*). Immunoblot analysis showed that MURC/Cavin-4 coimmunoprecipitated with phosphorylated and total ERK (Fig. 4*E*).

The stability of ERK proteins influences the duration of ERK activity (27). Thus, we evaluated the stability of phosphorylated and total ERK using cycloheximide (CHX), a protein biosynthesis inhibitor. The stability of phosphorylated and total ERK proteins was significantly increased following CHX treatment in MURC-expressing cardiomyocytes compared with the level in those expressing LacZ (Fig. S4*D*).

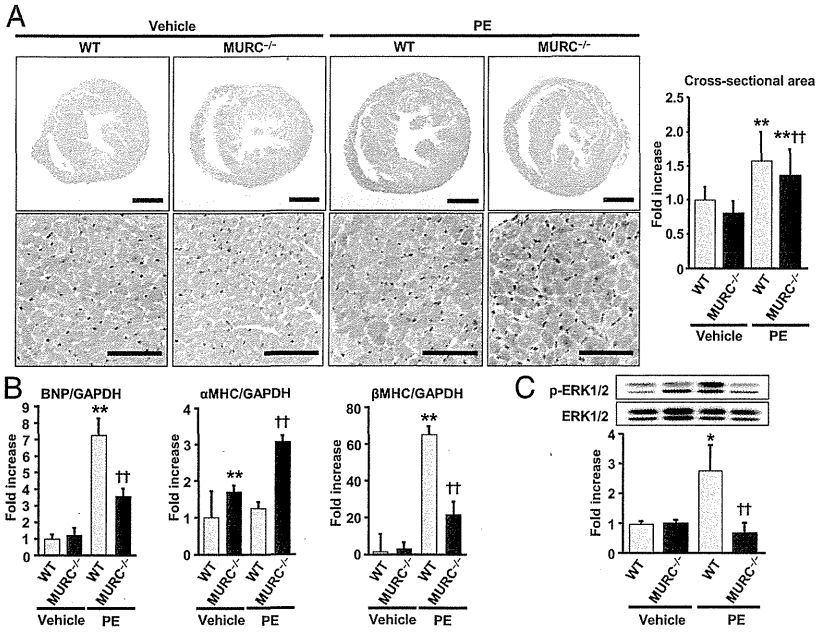

Fig. 3. MURC/Cavin-4 deletion attenuates α1-AR–induced ERK1/2 activation and cardiac hypertrophy. (*A*) Representative H&E staining of WT and *MURC*$^{-/-}$ heart paraffin-embedded sections (*A*, *Upper*, *Left*) and measurement of relative myocyte cross-sectional area (*A*, *Upper*, *Right*). WT and *MURC*$^{-/-}$ mice were infused with PE for 7 d with osmotic minipumps. Higher magnification images are shown (*Lower*). (Scale bars: 1 mm in *Upper*, and 50 μm in *Lower*.) A bar graph showing cross-sectional areas relative to vehicle-treated WT mice. (*B*) Measurements of BNP, αMHC, and βMHC mRNA levels in the heart. (*C*) Measurement of ERK1/2 activation in the heart. WT and *MURC*$^{-/-}$ mice were infused with PE for 2 d with osmotic minipumps. Data are presented as mean ± SEM. $^{*}P < 0.05$ and $^{**}P < 0.01$ compared with vehicle-treated WT mice; $^{\dagger\dagger}P < 0.01$ compared with PE-treated WT mice.

MURC/Cavin-4 Modulates α1-AR–Induced Cardiomyocyte Hypertrophy Through ERK Activation. We previously demonstrated cardiomyocyte hypertrophy in young MURC-Tg mice (11). In the present study, we found that ERK activity was increased in the cardiomyocytes of 6-wk-old MURC-Tg mice (Fig. 5*A*) and that MURC/Cavin-4 overexpression promoted cardiomyocyte hypertrophy (Fig. 5*B*). Furthermore, ERK1/2 siRNA knockdown (Fig. S5) significantly inhibited MURC/Cavin-4- and α1-AR–induced increase in cardiomyocyte size (Fig. 5 *C* and *D*). These results indicated that MURC/Cavin-4 was required for ERK activation in cardiomyocyte hypertrophy. ERK activity is regulated by MEK (28); therefore, to determine whether MURC/Cavin-4 modulates ERK activation through MEK1/2, we measured MEK1/2 activity in cardiomyocytes (Fig. S6). Under basal conditions, MURC/Cavin-4 overexpression did not affect MEK1/2 activation, whereas ERK was activated by MURC/Cavin-4 overexpression compared with LacZ. MEK1/2 activation in MURC/Cavin-4–overexpressing PE-stimulated cardiomyocytes was significantly enhanced compared with that in LacZ-overexpressing cardiomyocytes. In addition, ERK activation was synergistically enhanced by MURC/Cavin-4

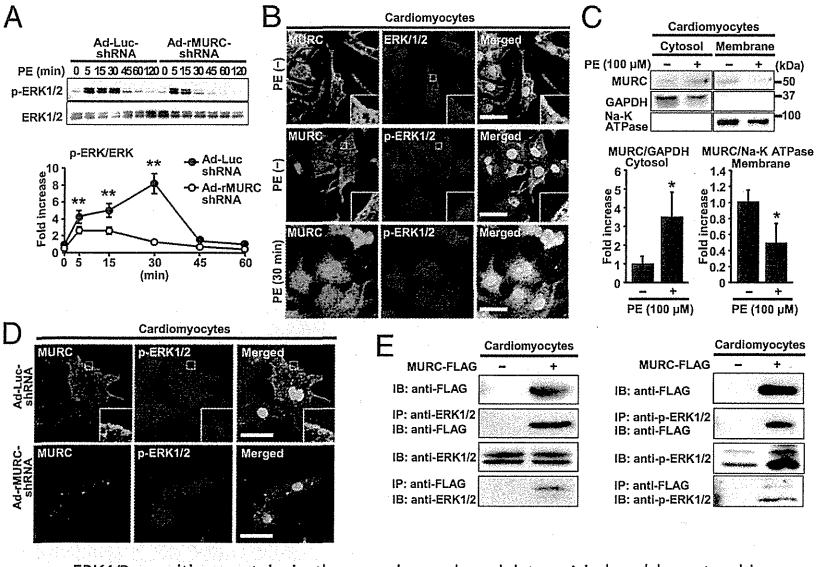

Fig. 4. MURC/Cavin-4 serves as an ERK1/2-recruiting protein in the caveolae and modulates α1-induced hypertrophic responses in cardiomyocytes. (*A*) Representative Western blots (*Upper*) and quantification of ERK phosphorylation (*Lower*) in cardiomyocytes with 100 μM PE. Data are presented as mean ± SEM. $^{**}P < 0.01$ compared with Ad-LucshRNA; $^{\dagger\dagger}P < 0.01$ compared with PE-treated Ad-Luc shRNA. (*B*) Representative immunostaining of ERK1/2 and MURC/Cavin-4 in cardiomyocytes. MURC/Cavin-4 was costained with ERK1/2 and p-ERK1/2 (white boxes). (*C*) Representative Western blots (*Upper*) and quantification of MURC protein levels in the cytosol and membrane fractions (*Lower*). Cells were treated with 100 μM PE for 30 min. (*D*) Representative immunostaining of p-ERK1/2 and MURC in MURC knocked-down cardiomyocytes. (Scale bars: 20 μm in *B* and *D*.) (*E*) Cell lysates were subjected to immunoprecipitation with anti-FLAG, anti-ERK1/2 (*Left*) and anti–p-ERK1/2 (*Right*) antibodies. Nuclei were stained with DAPI (blue).

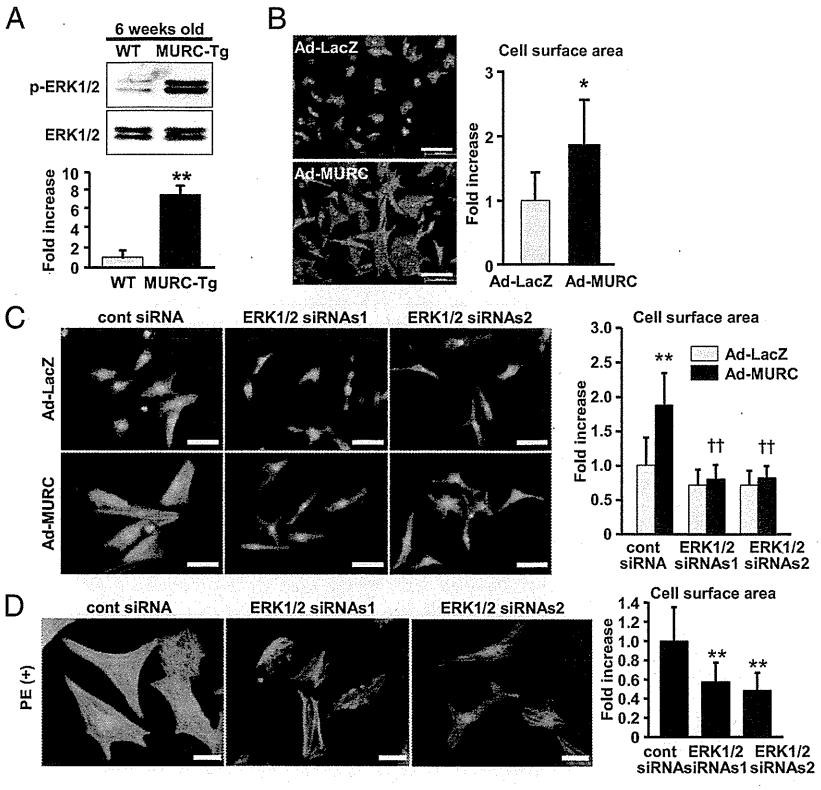

Fig. 5. MURC/Cavin-4 modulates α1-AR–induced cardiomyocyte hypertrophy through ERK1/2 activation. (*A*) Representative Western blots (*Upper*) and quantification of ERK1/2 phosphorylation (*Lower*) in 6-wk-old WT and MURC-Tg mice. $^{**}P < 0.01$ compared with WT mice. (*B*) Representative phalloidin-FITC–stained cardiomyocytes (*Left*) and quantification of cell surface area (*Right*). $^{*}P < 0.05$ compared with Ad-LacZ. (*C*) Representative fluorescence images of cardiomyocytes (*Left*) and quantification of cell surface area (*Right*). $^{**}P < 0.01$ compared with control siRNA-transfected Ad-LacZ; $^{\dagger\dagger}P < 0.01$ compared with control siRNA-transfected Ad-MURC. (*D*) Representative phalloidin-FITC–stained cardiomyocytes stimulated by PE. Cardiomyocytes were transfected with ERK1/2 siRNA and then stimulated by 100 μM PE for 48 h (*Left*), and cell surface area was quantified (*Right*). $^{**}P < 0.01$ compared with control siRNA. (Scale bars: 100 μm in *B*; and 50 μm in *C* and *D*.) All cells were stained by phalloidin-FITC. Nuclei were stained by DAPI (blue). ERK1/2 siRNAs1 indicates ERK1 siRNA-1 and ERK2 siRNA-1 cotransfection, and ERK1/2 siRNAs2 indicates ERK1 siRNA-2 and ERK2 siRNA-2 cotransfection. Data are presented as mean ± SEM.

overexpression in response to PE stimulation. Taken together, these findings suggested that MURC/Cavin-4 was capable of regulating ERK activation in a MEK1/2-dependent and -independent manner and that MURC/Cavin-4 served as a caveolar platform, thereby allowing activated α1-ARs to elicit MEK1/2 activation efficiently.

Discussion

Similar to caveolins, cavins are caveolar components that modulate caveolar morphology (29). Among the cavins, PTRF/Cavin-1 is required for caveola formation in various cell types including epithelium, smooth muscle, and skeletal muscle (16, 30). A recent study showed that SDPR/Cavin-2 deletion caused a pronounced reduction in caveola abundance in lung endothelium, but not in heart endothelium and that SRBC/Cavin-3 deletion did not affect caveolar formation in these cells (31). We demonstrated in the present study that MURC/Cavin-4 modified the morphology of formed caveolae in cardiomyocytes, whereas MURC/Cavin-4 was not essential to caveolar formation. Thus, all cavin proteins do not necessarily have the ability to form caveolae. Cav-3 KO mice showed a loss of caveolae in cardiomyocytes, leading to ERK activation and cardiac hypertrophy (19). We showed that Cav-3 knockdown reduced MURC/Cavin-4 localization at the plasma membrane, whereas MURC/Cavin-4 deficiency did not impair the membrane localization of Cav-3. Furthermore, unlike Cav-3 KO mice, MURC/Cavin-4–deficient mice exhibit normal caveolar morphology and function under physiological conditions. MURC/Cavin-4 deficiency attenuated ERK activation and cardiac hypertrophy induced by α1-AR stimulation. These results indicate that MURC/Cavin-4 regulates ERK activity and cardiac hypertrophy independently of caveolar morphology.

MURC/Cavin-4 bound to ERK1/2 in cardiomyocytes, and MURC/Cavin-4 and phosphorylated ERK were cotranslocated from the plasma membrane to the perinuclear region in response to PE. MURC/Cavin-4 knockdown attenuated PE-induced phosphorylated ERK accumulation at the plasma membrane. These findings suggest that MURC/Cavin-4 interacts with ERK and promotes ERK recruitment to caveolae and subsequent internalization by the caveolae. We also showed that MURC/Cavin-4 increased the stability of phosphorylated and total ERK proteins in cardiomyocytes, which suggests that MURC/Cavin-4 stabilized ERK proteins to prevent their inactivation and/or degradation, thereby sustaining ERK activation. Although scaffold proteins involved in ERK signaling, such as kinase suppressor of Ras (KSR), MAPK kinase (MEK) partner 1, MAPK organizer 1, and β-arrestin, have been identified (32), the relationship between these scaffolds and the caveolae has not been documented. Our results provide the unique documentation that MURC/Cavin-4 is a scaffold protein for ERK in caveolae and contributes to the stabilization of ERK activity in cardiomyocytes. Thus, MURC/Cavin-4 spatiotemporally regulates α1-AR–induced ERK activation in cardiomyocytes.

Several studies have demonstrated that α1-ARs were localized to the plasma membrane (19, 33, 34), whereas Wright et al. (35) showed that α1-ARs were located around or within the nucleus, but not on the plasma membrane, in adult mouse cardiomyocytes. Thus, controversy exists regarding the localization of α1-ARs in cardiomyocytes. Because of a lack of proper antibodies for α1-AR subtypes (21), we expressed fluorescent protein-tagged α1-ARs in cardiomyocytes and showed that α1A- and α1B-ARs were colocalized with MURC/Cavin-4 and Cav-3 at the plasma membrane and partly within the cytoplasm in cardiomyocytes. It has been revealed that many GPCRs form oligomeric complexes, as either homo- or heterooligomers, and that GPCR oligomerization has effects on ligand binding, receptor activation, desensitization, and trafficking, as well as receptor signaling (21). We showed that MURC/Cavin-4 enhanced MEK1/2 activation in response to PE stimulation in cardiomyocytes. Because MURC/Cavin-4 interacts with α1A- and α1B-AR, our observations raise the possibility that MURC/Cavin-4 might contribute to an increase in the accessibility between each of the α1-ARs, which leads to α1-AR oligomerization and promotes α1-AR signaling. A previous

study reported that MEK1 was distributed in caveolae (25). On the basis of this evidence, we predicted that MURC/Cavin-4 interacted with MEK1/2 as well as ERK in the caveolae, although coimmunoprecipitation analysis did not demonstrate an association between MURC/Cavin-4 and MEK1/2. Considering that MURC/Cavin-4 is colocalized with α1-ARs, MURC/Cavin-4 may also contribute to the functional compartmentation of α1-AR signaling of the caveolae, which facilitates the responsiveness of MEK1/2 activation in response to α1-AR stimulation, although MURC/Cavin-4 does not interact with MEK1/2 directly.

In cultured cardiomyocytes, ERK depletion using an antisense oligonucleotide was shown to down-regulate PE-induced hypertrophic responses (36). In the present study, ERK1/2 knockdown inhibited MURC/Cavin-4– and PE-induced cardiomyocyte hypertrophy. Thus, ERK has a crucial role in α1-AR– and MURC/Cavin-4–induced cardiac hypertrophy. Furthermore, MURC/Cavin-4 knockdown inhibited PE-induced cardiomyocyte hypertrophy associated with ERK inactivation. These findings suggested that MURC/Cavin-4 mediated PE-induced ERK signaling in cardiomyocytes.

Although the role of ERK signaling in cardiomyocyte hypertrophy is unknown (37), activated MEK1 induced concentric cardiac hypertrophy with ERK1/2 activation in transgenic mice (28). ERK1/2-deficient mice showed increases in the heart:body weight ratio and reductions in cardiac contractility under physiological conditions, which resulted in eccentric hypertrophy and cardiomyocyte elongation (38). Furthermore, angiotensin II and PE stimulation worsened eccentric cardiac growth in ERK1/2-deficient mice. However, in our present study, 1 wk of PE infusion inhibited concentric hypertrophy in *MURC*$^{-/-}$ mice, but did not promote eccentric hypertrophy, despite the inhibition of ERK activation. The discrepancy between these studies may be explained by a difference in the levels of suppressed ERK activity. Eccentric hypertrophy and cardiomyocyte elongation were observed in ERK1/2-deficient mice, which have complete loss of ERK activity (38). On the other hand, MURC/Cavin-4 deficiency maintained baseline ERK activity in the cardiomyocytes compared with that in control mice under physiological conditions. These observations suggested that concentric hypertrophy was modulated by ERK activation, which is induced by various stimuli, and that eccentric hypertrophy was modulated by a reduction in basal ERK activity.

As shown in the present study, although MURC/Cavin-4 is dispensable for caveolar formation in cardiomyocytes, MURC/Cavin-4 serves as an ERK-recruiting protein in the caveolae within cardiomyocytes. The recruiting function of MURC/Cavin-4 is necessary to elicit efficient signaling of the α1-AR/ERK cascade in the caveolae in concentric cardiac hypertrophy, which provides unique insight into the molecular mechanisms underlying caveola-mediated signaling in cardiac hypertrophy.

Materials and Methods

Pearson product-moment correlation coefficient was used to measure the linear correlation between variables. All experiments were performed at least thrice. Data are expressed as mean ± SEM and were analyzed by one-way ANOVA with post hoc analysis. A P value of <0.05 was considered significant.

The other materials and methods used for this study are described in *SI Materials and Methods*.

ACKNOWLEDGMENTS. We greatly appreciate Dr. H. Kasahara (University of Florida College of Medicine) for valuable suggestions. This work was supported by Grants-in-Aid from the Ministry of Education, Culture, Sports, Science, and Technology of Japan; the Japan Association for the Advancement of Medical Equipment; and the Takeda Science Foundation and the Mitsubishi Pharma Research Foundation.

1. Shaul PW, Anderson RG (1998) Role of plasmalemmal caveolae in signal transduction. *Am J Physiol* 275(5 Pt 1):L843–L851.
2. Parton RG, Simons K (2007) The multiple faces of caveolae. *Nat Rev Mol Cell Biol* 8(3): 185–194.
3. Razani B, Woodman SE, Lisanti MP (2002) Caveolae: From cell biology to animal physiology. *Pharmacol Rev* 54(3):431–467.
4. Cohen AW, Hnasko R, Schubert W, Lisanti MP (2004) Role of caveolae and caveolins in health and disease. *Physiol Rev* 84(4):1341–1379.
5. Harvey RD, Calaghan SC (2012) Caveolae create local signalling domains through their distinct protein content, lipid profile and morphology. *J Mol Cell Cardiol* 52(2): 366–375.
6. Hansen CG, Nichols BJ (2010) Exploring the caves: Cavins, caveolins and caveolae. *Trends Cell Biol* 20(4):177–186.
7. Briand N, Dugail I, Le Lay S (2011) Cavin proteins: New players in the caveolae field. *Biochimie* 93(1):71–77.
8. Williams TM, Lisanti MP (2004) The Caveolin genes: From cell biology to medicine. *Ann Med* 36(8):584–595.
9. Gratton JP, Bernatchez P, Sessa WC (2004) Caveolae and caveolins in the cardiovascular system. *Circ Res* 94(11):1408–1417.
10. Bastiani M, et al. (2009) MURC/Cavin-4 and cavin family members form tissue-specific caveolar complexes. *J Cell Biol* 185(7):1259–1273.
11. Ogata T, et al. (2008) MURC, a muscle-restricted coiled-coil protein that modulates the Rho/ROCK pathway, induces cardiac dysfunction and conduction disturbance. *Mol Cell Biol* 28(10):3424–3436.
12. Rodriguez G, et al. (2011) Molecular genetic and functional characterization implicate muscle-restricted coiled-coil gene (MURC) as a causal gene for familial dilated cardiomyopathy. *Circ Cardiovasc Genet* 4(4):349–358.
13. McMahon KA, et al. (2009) SRBC/cavin-3 is a caveolin adapter protein that regulates caveolae function. *EMBO J* 28(8):1001–1015.
14. Hayashi YK, et al. (2009) Human PTRF mutations cause secondary deficiency of caveolins resulting in muscular dystrophy with generalized lipodystrophy. *J Clin Invest* 119(9):2623–2633.
15. Bastiani M, Parton RG (2010) Caveolae at a glance. *J Cell Sci* 123(Pt 22):3831–3836.
16. Hill MM, et al. (2008) PTRF-Cavin, a conserved cytoplasmic protein required for caveola formation and function. *Cell* 132(1):113–124.
17. Hansen CG, Bright NA, Howard G, Nichols BJ (2009) SDPR induces membrane curvature and functions in the formation of caveolae. *Nat Cell Biol* 11(7):807–814.
18. Allen JA, Halverson-Tamboli RA, Rasenick MM (2007) Lipid raft microdomains and neurotransmitter signalling. *Nat Rev Neurosci* 8(2):128–140.
19. Woodman SE, et al. (2002) Caveolin-3 knock-out mice develop a progressive cardiomyopathy and show hyperactivation of the p42/44 MAPK cascade. *J Biol Chem* 277(41):38988–38997.
20. Jensen BC, Swigart PM, De Marco T, Hoopes C, Simpson PC (2009) α1-Adrenergic receptor subtypes in nonfailing and failing human myocardium. *Circ Heart Fail* 2(6):654–663.
21. Breitwieser GE (2004) G protein-coupled receptor oligomerization: Implications for G protein activation and cell signaling. *Circ Res* 94(1):17–27.
22. Fujita T, et al. (2001) Accumulation of molecules involved in alpha1-adrenergic signal within caveolae: Caveolin expression and the development of cardiac hypertrophy. *Cardiovasc Res* 51(4):709–716.
23. O'Connell TD, et al. (2003) The $\alpha_{(1A/C)}$- and $\alpha_{(1B)}$-adrenergic receptors are required for physiological cardiac hypertrophy in the double-knockout mouse. *J Clin Invest* 111(11):1783–1791.
24. Muslin AJ (2008) MAPK signalling in cardiovascular health and disease: Molecular mechanisms and therapeutic targets. *Clin Sci (Lond)* 115(7):203–218.
25. Liu P, Ying Y, Anderson RG (1997) Platelet-derived growth factor activates mitogen-activated protein kinase in isolated caveolae. *Proc Natl Acad Sci USA* 94(25):13666–13670.
26. Kholodenko BN, Hancock JF, Kolch W (2010) Signalling ballet in space and time. *Nat Rev Mol Cell Biol* 11(6):414–426.
27. Lu Z, Xu S, Joazeiro C, Cobb MH, Hunter T (2002) The PHD domain of MEKK1 acts as an E3 ubiquitin ligase and mediates ubiquitination and degradation of ERK1/2. *Mol Cell* 9(5):945–956.
28. Bueno OF, et al. (2000) The MEK1-ERK1/2 signaling pathway promotes compensated cardiac hypertrophy in transgenic mice. *EMBO J* 19(23):6341–6350.
29. Nabi IR (2009) Cavin fever: Regulating caveolae. *Nat Cell Biol* 11(7):789–791.
30. Liu L, et al. (2008) Deletion of Cavin/PTRF causes global loss of caveolae, dyslipidemia, and glucose intolerance. *Cell Metab* 8(4):310–317.
31. Hansen CG, Shvets E, Howard G, Riento K, Nichols BJ (2013) Deletion of cavin genes reveals tissue-specific mechanisms for morphogenesis of endothelial caveolae. *Nat Commun* 4:1831.
32. Dhanasekaran DN, Kashef K, Lee CM, Xu H, Reddy EP (2007) Scaffold proteins of MAP-kinase modules. *Oncogene* 26(22):3185–3202.
33. Petrashevskaya NN, Bodi I, Koch SE, Akhter SA, Schwartz A (2004) Effects of α1-adrenergic stimulation on normal and hypertrophied mouse hearts. Relation to caveolin-3 expression. *Cardiovasc Res* 63(3):561–572.
34. Koga A, et al. (2003) Adenovirus-mediated overexpression of caveolin-3 inhibits rat cardiomyocyte hypertrophy. *Hypertension* 42(2):213–219.
35. Wright CD, et al. (2008) Nuclear α1-adrenergic receptors signal activated ERK localization to caveolae in adult cardiac myocytes. *Circ Res* 103(9):992–1000.
36. Glennon PE, et al. (1996) Depletion of mitogen-activated protein kinase using an antisense oligodeoxynucleotide approach downregulates the phenylephrine-induced hypertrophic response in rat cardiac myocytes. *Circ Res* 78(6):954–961.
37. Kehat I, Molkentin JD (2010) Extracellular signal-regulated kinase 1/2 (ERK1/2) signaling in cardiac hypertrophy. *Ann N Y Acad Sci* 1188:96–102.
38. Kehat I, et al. (2011) Extracellular signal-regulated kinases 1 and 2 regulate the balance between eccentric and concentric cardiac growth. *Circ Res* 108(2):176–183.

DOI: 10.1111/joic.12002

STRUCTURAL HEART DISEASE

Long-Term Effects of Transcatheter Closure of Atrial Septal Defect on Cardiac Remodeling and Exercise Capacity in Patients Older than 40 Years with a Reduction in Cardiopulmonary Function

YOICHI TAKAYA, M.D.,[1] MANABU TANIGUCHI, M.D.,[2,3] TEIJI AKAGI, M.D.,[2] SAORI NOBUSADA, M.T.,[4] KENGO KUSANO, M.D.,[1] HIROSHI ITO, M.D.,[1] and SHUNJI SANO, M.D.,[2,5]

From the [1]Department of Cardiovascular Medicine, Okayama University Graduate School of Medicine, Dentistry and Pharmaceutical Sciences, Okayama, Japan; [2]Division of Cardiac Intensive Care Unit, Okayama University Hospital, Okayama, Japan; [3]Division of Cardiovascular Medicine, Fukuyama Cardiovascular Hospital, Fukuyama, Japan; [4]Division of Central Clinical Laboratory, Okayama University Hospital, Okayama, Japan; and [5]Department of Cardiovascular Surgery, Okayama University Graduate School of Medicine, Dentistry and Pharmaceutical Sciences, Okayama, Japan

Background: *Although it has been demonstrated that cardiac remodeling and exercise capacity improve after transcatheter closure of atrial septal defect (ASD), little is known about long-term benefits in middle-aged and elderly patients with a reduction in cardiopulmonary function.*

Objectives: *To evaluate long-term extent and time course of improvements in cardiac remodeling and exercise capacity in those patients.*

Methods: *Twenty ASD patients ≥ 40 years of age with a reduction in cardiopulmonary function (predicted peak oxygen uptake [VO_2] < 65%) were enrolled. Transthoracic echocardiography and cardiopulmonary exercise testing were performed at baseline and at 1 month, 3 months, 6 months, and >12 months after the procedure.*

Results: *At 1 month after the procedure, significant decreases in right ventricular (RV) end-diastolic diameter (38.2 ± 4.4 to 31.9 ± 4.4 mm; P < 0.001) and RV/left ventricular end-diastolic diameter ratio (0.95 ± 0.17 to 0.71 ± 0.13; P < 0.001) occurred, and they were maintained during the follow-up period. Normal RV size was achieved in 11 of 18 patients with RV enlargement. Predicted peak VO_2 did not change at 1 month and 3 months, but it improved significantly after 6 months (53.6 ± 6.5 to 62.1 ± 12.6%; P < 0.01). Sixteen of the 20 patients showed improved predicted peak VO_2.*

Conclusions: *Cardiac remodeling and exercise capacity could be improved over the long-term period after transcatheter closure of ASD in middle-aged and elderly patients with a reduction in cardiopulmonary function. There were differences in the time course of improvement between cardiac remodeling and exercise capacity in those patients.* (J Interven Cardiol 2013;26:195–199)

Introduction

Atrial septal defect (ASD) of secundum type is one of the most common forms of congenital heart disease in adults. Many patients with ASD are usually asymptomatic in early life, but clinical symptoms such as fatigue and dyspnea develop frequently in the course of time.[1,2] The development of clinical symptoms, echocardiographic signs of shunt volume or shunt-related pulmonary hypertension are widely accepted indications for closure of ASD. It is well known that surgical closure of ASD leads to long-term functional benefits in middle-aged and elderly symptomatic patients.[3–6] In recent years, transcatheter closure of ASD has been established as a secure and effective treatment, and it has become an important alternative to surgical repair for ASD.[7,8] A few studies

Conflict of interest: None

Address for reprints: Manabu Taniguchi, M.D., 2–39 Midorimachi, Fukuyama-shi, Hiroshima 720-0804, Japan. Fax: +81-84-925-9650; e-mail: tmnb@hotmail.com

have shown short-term benefits of transcatheter closure of ASD on cardiac remodeling and exercise capacity in middle-aged and elderly patients.[9,10] However, little is known about long-term results. Furthermore, the extent and time course of functional improvements after the procedure in middle-aged and elderly patients with a marked reduction in cardiopulmonary function remains unclear. Therefore, the aim of this study was to investigate the long-term extent and time course of improvements in cardiac remodeling and exercise capacity after transcatheter closure of ASD in those patients.

Methods

Study Population. From June 2006 to April 2009, 20 consecutive ASD patients $\geq$ 40 years of age with a moderate or severe reduction in cardiopulmonary function who underwent transcatheter closure of secundum ASD were enrolled. We defined moderate reduction in cardiopulmonary function as 50% $\leq$ predicted peak oxygen uptake (VO_2) < 65%, and we defined severe reduction as predicted peak VO_2 < 50%. The indications for ASD closure in all patients were significant left-to-right shunt detected by echocardiography, presence of right ventricular (RV) volume overload, shunt-related symptoms, or pulmonary hypertension. Exclusion criteria included pulmonary vascular resistance > 8 wood units on 100% O_2 and transesophageal maximal ASD diameter > 40 mm. The Okayama University Ethics Committee approved this study, which was performed in accordance with the Helsinki declaration, and all patients provided written informed consent before participation in this study.

Transcatheter Closure of ASD. Transesophageal echocardiography was performed in all patients before the procedure, and left atrial thrombi were not detected in any of the patients. Coronary angiography was performed in all patients, and there was no significant coronary stenosis. Transcatheter closure of ASD using an AMPLATZER septal occluder device (AGA Medical Corporation; Plymouth, MN, USA) was performed under general anesthesia with the assistance of transesophageal echocardiography. Hemodynamic evaluation was performed just before ASD closure. With oxygen uptake measured at rest, the pulmonary to systemic flow ratio was calculated by oxymetry using the Fick principle. If the pulmonary wedge pressure increased > 5 mmHg from baseline, the procedure was abandoned.

Echocardiography. Transthoracic echocardiography was performed at baseline and at 1 month, 3 months, 6 months, and >12 months after the procedure using a 3.5 MHz transducer (Aplio, Toshiba, Otawara, Japan). Left ventricular (LV) end-diastolic diameter, LV end-systolic diameter, and RV end-diastolic diameter were measured by M-mode parasternal echocardiography, and RV/LV end-diastolic diameter ratio was calculated. LV ejection fraction was derived using Teichholz's formula. These measurements were done at least three times and averaged to obtain mean values by 2 independent experienced investigators who were blinded to the data of treatment.

Cardiopulmonary Exercise Testing. Cardiopulmonary exercise testing was performed at baseline and at 1 month, 3 months, 6 months, and >12 months after the procedure. All patients underwent symptom-limited exercise tests on an upright bicycle ergometer using a ramp protocol (15 W/min) with simultaneous respirator gas analysis. Patients were encouraged to exercise to exhaustion or to a respiratory exchange ratio $\geq$ 1.09. Blood pressure and heart rate were measured every minute. A 12-lead electrocardiogram was continuously monitored during exercise testing. Breathed gas was continuously collected to analyze VO_2, carbon dioxide production, and minute ventilation with a gas analyzer. Peak VO_2 was defined as the highest VO_2 value achieved at peak exercise after reaching the respiratory compensation point, and predicted peak VO_2 was expressed according to age, sex, weight, and height. VO_2 to work rate ratio ($\Delta VO_2/\Delta WR$) was determined. A spirometric measurement was performed to assess vital capacity and forced expiratory volume in 1 second. These analyses were done by 2 independent experienced investigators who were blinded to the data of treatment.

Statistical Analysis. Variables are expressed as means $\pm$ standard deviation or percentage. Statistical analysis was performed by Wilcoxon's matched-pairs test. A P value < 0.05 was considered to be statistically significant.

Results

Study Population. Patient clinical characteristics are summarized in Table 1. Mean age at transcatheter closure of ASD was 54.5 $\pm$ 10.9 years (range, 40–78 years). Fourteen patients (70%) were female. ASD diameter measured by transesophageal echocardiography was 17.8 $\pm$ 4.3 mm. Pulmonary to

Table 1. Patient Clinical Characteristics

Variables	
Age (years)	54.5 ± 10.9
Female (%)	70
Smoking (%)	25
Lung disease (%)	15
Hypertension (%)	25
Diabetes mellitus (%)	10
Stroke (%)	5
Atrial septal defect diameter (mm)	17.8 ± 4.3
Device size (mm)	21.7 ± 4.7
Pulmonary to systemic flow ratio	2.6 ± 0.6
Mean pulmonary artery pressure (mmHg)	14.5 ± 4.0
Vital capacity (l)	2.9 ± 0.6
Forced expiratory volume in 1 second (l/second)	2.3 ± 0.6

Data are presented as mean ± standard deviation or percentage.

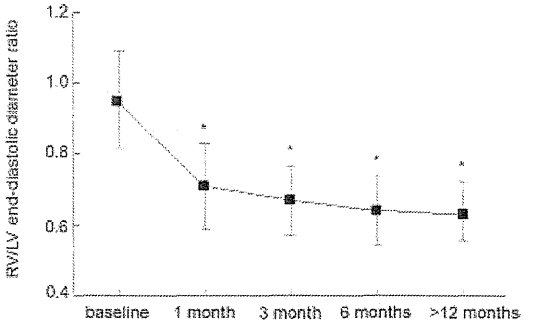

Figure 1. Time course of data on RV/LV end-diastolic diameter after transcatheter closure of atrial septal defect. *P < 0.001 versus baseline. RV = right ventricular; LV = left ventricular.

systemic flow ratio was 2.6 ± 0.6, and mean pulmonary artery pressure under general anesthesia was 14.5 ± 4.0 mmHg. Transcatheter closure of ASD was performed successfully in all patients using an AMPLATZER septal occluder device. All patients were followed up for a mean period of 25.2 ± 10.5 months (range, 12.0–40.8 months). There were no complications including thromboembolic events in the procedural and follow-up period.

Cardiac Remodeling and Exercise Capacity. Time courses of data obtained by transthoracic echocardiography and cardiopulmonary exercise testing at baseline and after the procedure are summarized in Table 2. At baseline, RV enlargement (RV end-diastolic diameter >30 mm) was present in 18 patients (90%). After the procedure, a significant decrease in RV end-diastolic diameter was observed at 1 month, and it was maintained during the follow-up period. Eleven of 18 patients with RV enlargement (61%) achieved a normal RV size (RV end-diastolic diameter <30 mm). In addition, LV end-diastolic diameter increased significantly. Therefore, cardiac remodeling resulted in a decrease in RV/LV end-diastolic diameter ratio at 1 month (Fig. 1). LV ejection fraction and LV end-systolic diameter did not change from baseline. At baseline, 13 patients (65%) had a moderate reduction in cardiopulmonary function and 7 patients (35%) had a severe reduction. After the procedure, predicted peak VO_2 did not change at 1 month and 3 months, but it improved significantly after 6 months (Fig. 2). Predicted peak VO_2 increased overall by 15%, and 16 of the 20 patients (80%), including 10 of the 13 patients with a moderate reduction in cardiopulmonary function and 6 of the 7 patients with a severe reduction in cardiopulmonary function, showed improved predicted peak VO_2 in the follow-up period. In addition, a

Table 2. Transthoracic Echocardiography and Cardiopulmonary Exercise Testing at Baseline and After Transcatheter Closure of Atrial Septal Defect

Variables	Baseline	1 month	3 months	6 months	>12 months
LV end-diastolic diameter (mm)	40.7 ± 5.0	45.7 ± 5.3**	46.1 ± 4.7**	46.5 ± 5.3**	46.6 ± 5.2***
LV end-systolic diameter (mm)	24.4 ± 3.9	26.9 ± 3.7	26.2 ± 3.1	26.8 ± 3.9	26.8 ± 3.6
LV ejection fraction (%)	71.2 ± 5.2	72.3 ± 4.0	74.0 ± 4.4	73.4 ± 5.4	73.6 ± 4.7
RV end-diastolic diameter (mm)	38.2 ± 4.4	31.9 ± 4.4***	30.5 ± 3.5***	29.6 ± 3.2***	29.3 ± 2.9***
RV/LV end-diastolic diameter ratio	0.95 ± 0.17	0.71 ± 0.13***	0.67 ± 0.10***	0.64 ± 0.10***	0.63 ± 0.08***
Predicted peak oxygen uptake (%)	53.6 ± 6.5	55.8 ± 11.5	56.8 ± 9.7	62.1 ± 12.6**	61.8 ± 9.7**
Peak oxygen uptake (ml/min/kg)	15.4 ± 2.3	16.3 ± 3.7	16.0 ± 2.9	17.6 ± 3.9*	17.5 ± 3.5*
Oxygen uptake to work rate ratio	7.3 ± 1.8	6.9 ± 1.6	7.9 ± 1.6	8.1 ± 1.7	8.3 ± 1.4*

Data are presented as mean ± standard deviation.
*P < 0.05 versus baseline, ** P < 0.01 versus baseline, *** P < 0.001 versus baseline.
LV = left ventricular; RV = right ventricular.

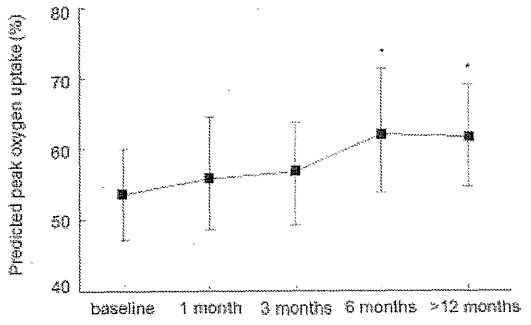

Figure 2. Time course of data on predicted peak oxygen uptake after transcatheter closure of atrial septal defect. *P < 0.01 versus baseline.

significant improvement in $\Delta VO_2/\Delta WR$ was observed at > 12 months after the procedure.

Discussion

In this study, we evaluated long-term functional benefits of transcatheter closure of ASD in middle-aged and elderly patients with a marked reduction in cardiopulmonary function, and we found significant improvements in cardiac remodeling and exercise capacity. Decrease or even normalization of RV size and RV/LV end-diastolic diameter ratio occurred early after the procedure, and they were maintained during the long-term period. Exercise capacity measured by cardiopulmonary exercise testing did not change early, but it improved during the long-term period. We also found the time delay of improvement in exercise capacity compared with cardiac remodeling in those patients. The severity of functional limitation increases with advancing age in the majority of patients with ASD.[1,2] The clinical courses and long-term results after surgery depend mainly on the patient's preoperative clinical status. In the past, controversy existed as to whether middle-aged and elderly patients benefit from surgery. Murphy et al.[11] proved that symptomatic patients who undergo surgery after the age of 40 years were at increased risk for postoperative cardiovascular complications, whereas young adults had an excellent prognosis. However, several studies have demonstrated long-term benefits of surgical ASD closure in middle-aged and elderly symptomatic patients.[3–6] Konstantinides et al.[3] showed that surgical ASD closure in symptomatic patients over the age of 40 years increased long-term survival and prevented deterioration of New York Heart Association (NYHA) functional class during a follow-up period of 8.9 years. Jemielity et al.[4], in patients aged 40–62 years and followed for 6.9 years, also found a significant improvement in functional class with 61.8% patients in NYHA functional class III and IV before surgery compared with 82.4% in NYHA functional class I and II after surgery. These studies indicated that surgical ASD closure benefits many or most middle-aged and elderly symptomatic patients in the long-term period and therefore it is widely recommended for those patients. Recently, transcatheter closure of ASD has been performed safely and effectively, and it has become an alternative to surgical ASD closure.[7,8] Similar to surgical repair, several studies have demonstrated functional benefits of transcatheter closure of ASD in adult patients.[12–15] Giardini et al.[12] evaluated long-term impacts of transcatheter closure of ASD on RV remodeling and exercise capacity in asymptomatic patients, and they found a significant decrease in RV diameter and a significant improvement in peak VO_2. In comparison with this study, their study population was younger and had less severe cardiopulmonary function at the time of the procedure. Our study population consisted of only patients ≥ 40 years of age with a marked reduction in cardiopulmonary function to investigate patients considered at higher risk for functional recovery after the procedure. Regarding middle-aged and elderly patients, Brochu et al.[9] investigated results in asymptomatic or mildly symptomatic patients over the age of 40 years, and they showed that peak VO_2 was increased significantly at 6 months after the procedure. Jategaonkar et al.[10] reported a significant decrease in RV end-diastolic diameter and significant improvements of NYHA functional class and peak VO_2 at 3 months after the procedure even in patients over the age of 60 years. However, little is known about long-term results in those patients. Furthermore, although impaired exercise capacity is a predictive parameter in terms of mortality in congenital heart disease,[16,17] limited information is available for long-term extent of functional improvement in middle-aged and elderly patients with markedly reduced cardiopulmonary function. The recently published study of Khan et al.[18] showed significant improvements in cardiac remodeling and 6-min walk test at 12 months after the procedure in patients over the age of 40 years. Our results are similar to their findings. However, we also evaluated the time course of functional improvements, and we revealed that an improvement in exercise capacity was delayed compared with cardiac remodeling in middle-aged and elderly patients with a marked reduction in cardiopulmonary function. The mechanism leading to improved exercise capacity after the

procedure has been clarified. ASD closure with abolishment of left-to-right shunt leads to augmented LV filling by increased preload and therefore to improved stroke volume.[14] The rise in cardiac output may explain the increase of exercise capacity. In this study, we found the time delay of improvement in exercise capacity compared with cardiac remodeling. In addition, even if RV size was normalized in more than half of all patients, mean exercise capacity continued to be at least moderately reduced. Exercise capacity is influenced by several factors, not only cardiac output but also noncardiac factors such as pulmonary function and skeletal muscle function. We speculated that the delay of improvement in exercise capacity could be related to the time needed for the recover of skeletal muscle function after transcatheter closure of ASD in middle-aged and elderly patients with a marked reduction in cardiopulmonary function, but not the time needed for the recover of cardiac function. Similar to our results, Helber et al.[19] showed the lack of improvement in exercise capacity early after surgical ASD closure in patients over the age of 40 years, and they suggested that the improvement in exercise capacity took place after 1–2 years after the procedure. Thus, exercise training after the procedure may be needed to recover the pulmonary function and skeletal muscle function early in those patients.

Study Limitations. This study had some limitations. First, the current findings need confirmation in large studies because this study included only 20 patients from a single center. Second, exercise capacity is also influenced by noncardiac factors, but measurements of those factors are lacking. Finally, the evaluation of RV function using two-dimensional strain echocardiography, three-dimensional echocardiography, or tricuspid annular plane systolic excursion should be preferable to demonstrate RV remodeling after transcatheter closure of ASD.

Conclusion

Transcatheter closure of ASD in patients $\geq$ 40 years of age with markedly reduced cardiopulmonary function resulted in significant long-term improvements of cardiac remodeling and functional capacity. There were differences in the time course of improvement between cardiac remodeling and exercise capacity after the procedure in those patients.

References

1. Fredriksen PM, Veldtman G, Hechter S, et al. Aerobic capacity in adults with various congenital heart disease. Am J Cardiol 2001;87:310–314.
2. Markmann P, Howitt G, Wade EG. Atrial septal defect in the middle-aged and elderly. Quant J Med 1965;34:409–426.
3. Konstantinides S, Geibel A, Olschewski M, et al. A comparison of surgical and medical therapy for atrial septal defect in adults. N Engl J Med 1995;333:469–473.
4. Jemielity M, Dyszkiewicz W, Paluszkiewicz L, et al. Do patients over 40 years of age benefit from surgical closure of atrial septal defects? Heart 2001;85:300–303.
5. Nasrallah AT, Hall RJ, Garcia E, et al. Surgical repair of atrial septal defect in patients over 60 years of age. Long-term results. Circulation 1976;53:329–331.
6. Sutton MG, Tajik AJ, McGoon DC. Atrial septal defect in patients aged 60 years or older: Results and long-term postoperative follow-up. Circulation 1981;64:402–409.
7. Masura J, Gavora P, Formanek A, et al. Transcatheter closure of secundum atrial septal defects using the new self-centering amplatzer septal occluder: Initial human experience. Cathet Cardiovasc Diagn 1997;42:388–393.
8. Masura J, Gavora P, Podnar T. Long-term outcome of transcatheter secundum-type atrial septal defect closure using Amplatzer septal occluders. J Am Coll Cardiol 2005;45:505–507.
9. Brochu MC, Baril JF, Dore A, et al. Improvement in exercise capacity in asymptomatic and mildly symptomatic adults after atrial septal defect percutaneous closure. Circulation 2002;106:1821–1826.
10. Jategaonkar S, Scholtz W, Schmidt H, et al. Percutaneous closure of atrial septal defects: Echocardiographic and functional results in patients older than 60 years. Circ Cardiovasc Interv 2009;2:85–89.
11. Murphy JG, Gersh BJ, McGoon MD, et al. Long term outcome after surgery repair of isolated atrial septal defects. Follow-up at 27 to 32 years. N Engl J Med 1990;323:1645–1650.
12. Giardini A, Donti A, Specchia S, et al. Long-term impact of transcatheter atrial septal defect closure in adults on cardiac function and exercise capacity. Int J Cardiol 2008;124:179–182.
13. Veldtman GR, Razack V, Siu S, et al. Right ventricular form and function after percutaneous atrial septal defect device closure. J Am Coll Cardiol 2001;37:2108–2113.
14. Giardini A, Donti A, Formigari R, et al. Determinants of cardiopulmonary function improvement after transcatheter atrial septal defect closure in asymptomatic adults. J Am Coll Cardiol 2004;43:1886–1891.
15. Schoen SP, Kittner T, Bohl S, et al. Transcatheter closure of atrial septal defects improves right ventricular volume, mass, function, pulmonary pressure, and functional class: A magnetic resonance imaging study. Heart 2006;92:821–826.
16. Diller GP, Dimopoulos K, Okonko D, et al. Exercise intolerance in adult congenital heart disease: Comparative severity, correlates, and prognostic implication. Circulation 2005;112:828–835.
17. Giardini A, Specchia S, Berton E, et al. Strong and independent prognostic value of peak circulatory power in adults with congenital heart disease. Heart 2007;154:441–447.
18. Khan AA, Tan JL, Li W, et al. The impact of transcatheter atrial septal defect closure in the older population: A prospective study. JACC Cardiovasc Interv 2010;3:276–281.
19. Helber U, Baumann R, Seboldt H, et al. Atrial septal defect in adults: Cardiopulmonary exercise capacity before and 4 months and 10 years after defect closure. J Am Coll Cardiol 1997;29:1345–1350.